Tribology International Vol. 31, No. 6, pp. 313–323, 1998

Printed in Great Britain
0301–679X/98/$19.00 + 0.00

PII: S0301–679X(98)00040–1

Measurements of tribological properties of poly(pyrrole) thin film bearings

X. Liu*†, D. G. Chetwynd‡, J. W. Gardner‡, P. N. Bartlett§ and C. Beriet§

We report the results of a recent study on the tribological properties of electropolymerised thin films at light loads and low speeds. Poly(pyrrole) films incorporating different counter-ions have been electrochemically deposited onto gold electrodes on the plano-convex glass substrates and studied extensively. The measuring apparatus has been greatly improved from that reported earlier and now provides simultaneous monitoring of frictional force and wear. High precision capacitive gauging is employed to provide high resolutions of frictional force of better than 100 μN and height variation (wear) of 2 nm. A large number of specimens of poly(pyrrole) grown from five different counter-ions were prepared and their performances evaluated. The film morphology of each type of film was examined by atomic force microscopy (AFM) for control of the variability of film formation. Results are presented for the friction coefficients and wear rates observed for the films typically at a load of 2 N and a sliding speed of 5 mm s^{-1}. The effects of normal loading force and sliding speed on the friction coefficient are also discussed with a load range of 0.2–5 N and a sliding speed up to 30 mm s^{-1}.

Keywords: *capacitive sensing, conductive polymer, friction testing, polypyrrole films, precision bearing, surface characterisation*

Introduction

Nanotechnology and metrology are creating an ever-increasing demand for super-precision translations which require smooth and low friction between mechanically sliding parts[1,2]. Thin film lubrication has been favourable for such applications as it offers low friction and the thermal conductivity and contact stiffness are little affected by the presence of the film[3]. Polymeric thin film bearings, which slide dry against optically polished glass datums have been studied previously in high precision linear and angular slideways[4]. Generally, this has been achieved using a polytetrafluorethene (PTFE)–lead composite bearing contained within a sintered bronze matrix. PTFE is of particular interest for precision slideways because it consists of straight, long-chain, fluorocarbon molecules having a high stiffness perpendicular to the direction of sliding and low shear strength parallel to it. However, the bulk material has very little strength and its high creep rate and a high thermal expansion coefficient are also undesirable. In general, the PTFE bearings are formed in a polymer-metal matrix where lubrication is believed to be through orientated films being drawn from the matrix and deposited onto the metal (bronze) and counterface material. This mechanism has the intrinsic advantages that thermal conductivity and stiffness of the bearing are not adversely affected by the polymer, and wear is in part compensated by the reservoir held in the matrix. A disadvantage of this approach arises from the limited range of geometries to which such bearing

*School of Engineering, Coventry University, Coventry CV1 5FB, UK
†Corresponding author. Tel: + 44 1203 838 810; Fax: + 44 1203 838 272; E-mail: x.liu@coventry.ac.uk
‡Centre for Nanotechnology and Microengineering, Department of Engineering, University of Warwick, Coventry CV4 7AL, UK
§Department of Chemistry, University of Southampton, Southampton SO17 1BJ, UK
Received 20 November 1997; revised 12 May 1998; accepted 2 July 1998

pads can be applied realistically. Other applications of PTFE require relatively difficult deposition processes, which again tends to limit their use to simple geometric forms. Recent developments of molecular engineering have led to new organic conducting materials, including electroactive conducting polymers, which can be produced by the electrochemical polymerisation of suitable monomers in either aqueous or non-aqueous solutions. Distinct advantages of this technique are that the process is simple and easy to control, very thin films can be produced onto irregular surfaces, and films so formed have good thermal and chemical stability. Earlier research on conductive polymers such as poly(*N*-methypyrrole), poly(aniline), poly(5-carboxyindole) and poly(pyrrole) showed that a wide range of friction coefficients can be obtained by the choice of monomer, counter-ion, solvent, film thickness and growth potential[5,6]. A systematic study on poly(pyrrole) films has been concentrated in optimising the polymerisation processes for better tribological properties. Poly(pyrrole) was chosen as a model polymer system because it was found to give films with a wide range of friction coefficients depending on the choice of deposition conditions and counter-ion. In certain cases, a pyrrole-based film can have a friction coefficient comparable to or even better than that of PTFE. All the tests have been carried out using the modified friction test apparatus with improved instrumentation. A large set of experiments has been carried out in order to identify parametric relationships between the tribological properties of the films and the polymer type and structure. Film topography has been examined by atomic force microscopy (AFM) for thin films and scanning electron microscopy (SEM) for thick films.

Test apparatus and instrumentation

Design of the apparatus

The present apparatus design is based on an earlier friction test-rig[5] in that it uses a horizontal glass disc against which specimens are dead-weight loaded and an aluminium monolithic flexure mechanism, which supports the specimen and also measures the frictional force through its slight displacement. Improved sensitivity has been obtained by using capacitive micrometry, and a means to measure the wear of the film being tested has been introduced. The conventional method of weighing mass loss after operation is not suitable here as the thickness of films is no more than a few micrometres and the change is a minute fraction of the total specimen mass. Thus wear is monitored in-process by measuring relevant specimen height variation to indicate wear rate. The photograph and its schematic diagram of the modified apparatus is shown in Fig 1(a,b). It comprises a rotating optically flat glass disk driven by the DC motor with a gear box of 135:1 and a tachometer, the sample assembly that has a sample holder mechanism and a height probe for wear measurement, the parallel-spring flexure with a capacitive sensor to measure frictional force, and the ball-bearing support lever and a weight for setting the normal loading force. Details of the sample assembly are shown in Fig 2. The bearing specimen is glued on an aluminium bar which is held kinematically (seven balls) by a hinge-operated screwlock. With this kinematic mount the test specimen can be repositioned close to the same spot. The sample holder is designed for testing a four-bearing-pad specimen, and the aluminium bar can be turned so that each bearing film can be tested. Note from Fig 1 that the specimen holder is tilted for this purpose. The vertical probe is a type of capacitive sensor formed from the electrodes of a Zerodur glass base and a glass cantilever of 8.5 $\times$ 1.5 $\times$ 0.1 mm. A sapphire ball of 1 mm in diameter is glued onto the free end of the cantilever and will contact the rotating disk during operation. The vertical probe is mounted on a ceramic base, which is, in turn, mounted on the sample assembly via a triangular aluminium bar. This bar is held against six steel balls on the assembly base by elastic bands to approximate closely an ideal force-closed kinematic mount. The probe mount can be adjusted up to 1 mm in height by a screw-driven wedge working against the balls of the kinematic mount. Once it is positioned in place, that is in contact with the rotating plate with a contact force about 200 nN, the probe is then decoupled from the screw to improve thermal stability. The frictional force is measured by another capacitive sensor, which has one flat electrode attached to the sidewall of the moving platform of the spring flexure, and a spherical electrode on an aluminium rod, which is in turn locked to the base of the flexure. The spherical shape of the electrode reduces tilt sensitivity and thus allows the electrode be repositioned without the need of recalibration. The capacitances from both sensors are measured by capacitance gauges, NS2000 from Queensgate Instruments Ltd., which can measure changes equivalent to spacings of 0.1 nm in our configuration.

In general the apparatus is operated by a computer via a data acquisition card. Signals of frictional force, height variation and sliding speed are measured and the motor is driven by a single digital to analogue (D/A) channel via home-built power drive circuitry.

Calibrations

Friction probe

The friction sensor was calibrated directly against a set of standard weights by mounting the flexure in vertical position. Non-linearity associated with the capacitive sensors was balanced against their sensitivity. The smaller the capacitor's nominal gap the higher the sensitivity but the greater the non-linearity. Therefore a sensitivity of 0.428 N V^{-1} with 1% non-linearity was chosen for all the experiments. The resolution for frictional force measurement is the combination of the stiffness of the spring flexure and the sensitivity of the capacitive sensor and, with the present setting, the resolution is better than 0.1 mN.

Vertical probe

In operation the vertical probe monitors a height variation consisting of two parts; one is associated with the run-out of the rotating disk and the other corresponds to the wear of the film being tested. To reduce this run-

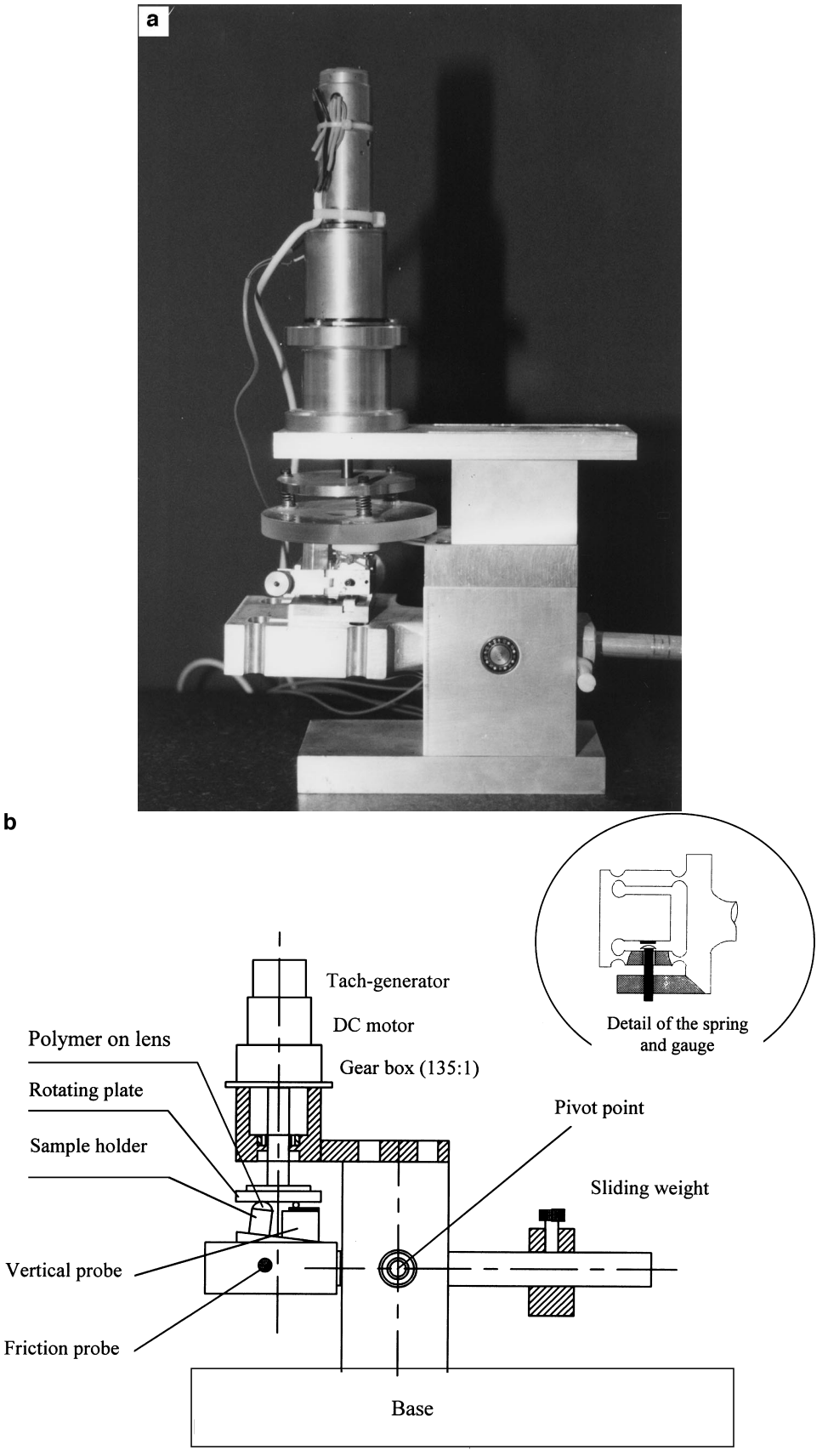

Fig. 1 (a) The photograph of the modified friction and wear test apparatus. (b) General schematic diagram of the modified friction and wear test apparatus

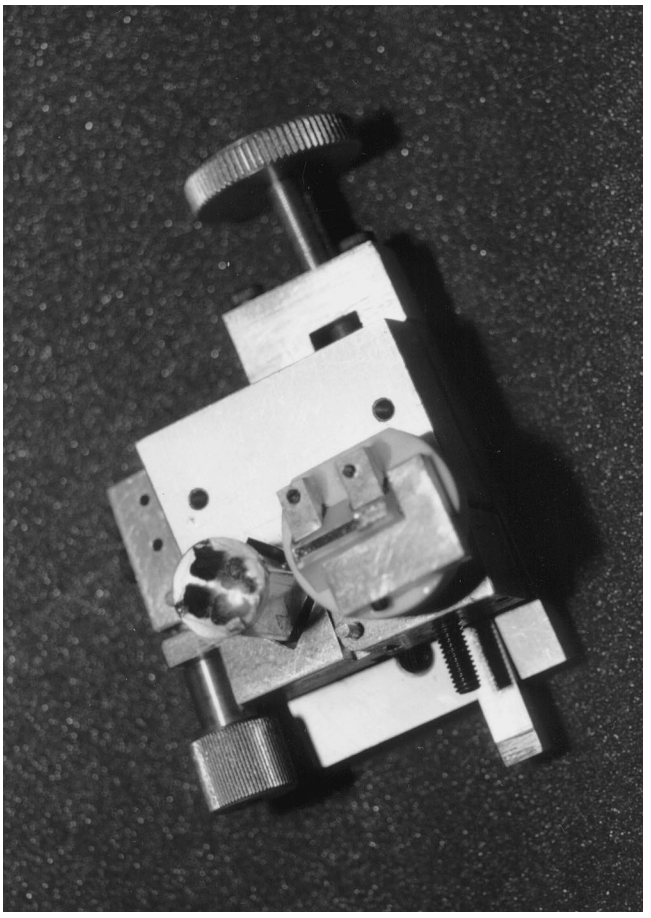

Fig. 2 The top view of the sample assembly mechanism

out variation, the vertical probe is mounted as close as possible to the centre of the rotation plate. Residual run-out can be discriminated from wear since it is periodic with disc rotation. The vertical probe has a nominal gap spacing of 20 μm, and is calibrated by a digital controlled piezoelectric translator (DPT; Queensgate Instruments Ltd.) with a resolution of 0.5 nm and factory certified accuracy traced to laser interferometry. Within the range of the displacement used the sensor has a linear response with a sensitivity of 9.731 μm V^{-1} and a standard deviation to the least squares straight line fitting of 0.002. Taking other factors into account the resolution for height variation measurement is better than 2 nm.

Contact force

Different normal forces are applied by sliding the counter-weight along the balance bar and the positions were calibrated by a set of standard weights. During the calibration, a standard weight was hung in line with the centre of the sample holder by a piece of string, then the counter was moved along the bar to locate the balance position. Repeating the procedure at a different weight (10, 20, 50, 100, 200, 350 and 500 g available), the normal loading force was calibrated from 0.098 to 4.91 N.

Stability

Thermal drifts on the two capacitive probes are very small due to the thermal properties of Zerodur material and the monolithic mechanism. Typical values are 3 mV/h for the friction sensor and less than 2 mV/h for the vertical probe. A better stability can be obtained after the system is powered on for several hours. Spurious vibration is not significant because the spring flexure is fairly stiff, possesses a large inertia, and works in a contact condition which leads to a large damping of the spring system.

Specimen surface analysis

Preparation of specimens

The bearing specimen consists of a plano-convex glass lens with a radius of 21.6 mm and a thickness of 3 mm. Tolerances on those dimensions are not critical and standard commercial lenses are used. It carries four heart-shaped metal electrodes, each having an area about 12 mm^2, comprising a 20 nm chromium adhesion layer followed by 200 nm of gold (Marz grade). Polymer films were then electrochemically deposited onto each electrode in turn. This could allow virtually identical films to be produced on a single lens and provides flexibility for the study of post-deposition conditioning.

A standard cleaning procedure was developed because the cleanliness of the glass substrate greatly affected the adhesion of the gold electrode onto the glass and thus the ability to electrodeposit reliably the polymer film. Specimens were cleaned in iso-proponal in an ultrasonic bath for 1 h, rinsed thoroughly, then washed in de-ionised distilled water in the ultrasonic bath, finally rinsed and dried with a stream of argon and stored in a desiccator for polymerisation.

Over 200 specimens were produced by electropolymerisation of poly(pyrrole) from different counter-ion, deposition potential, and film thickness. An aqueous solution of 0.1 mol dm^{-3} of pyrrole (purified by passage down an alumina column) and 0.1 mol dm^{-3} of the appropriate electrolyte was used and the deposition cell was kept at a constant temperature of 20 or 30°C for certain types of films. The poly(pyrrole) film was grown on each electrode by stepping the potential from 0 V against saturated calomel electrode (SCE) to a suitable growth potential (typically around + 0.6 V) using a commercial potentiostat (EG and G). Some polymer films were grown by a double potential step; the potential was first stepped to a higher voltage for a short period of time to create more nucleation sites and it was then stepped down to the normal value to carry out the growth more slowly. In both cases, the final oxidation state of the film was set by holding a potential of about + 0.3 V as the substrate was removed from the electrolyte.

All the polymers were grown in an aqueous solution with five different counter-ions; namely toluene sulfonic acid sodium salt (TSA), dodecylbenzene sulfonic acid sodium salt (DBSA), decane phosphonic acid (DPA), methane phosphonic acid (MPA), and butane phosphonic acid (BPA). Films were grown to an esti-

mated thickness (based on the charge transferred) that ranged from 30 nm to 5.2 μm. Generally, these films appear smooth and shiny to the naked eye. In the case of DPA, the solubility of the counter-ion was low and the solution was very viscous even at a higher temperature. Therefore the deposition was carried out at a constant temperature of 30°C for DPA and 20°C for the other counter-ions.

Surface morphology

Specimens were characterised by AFM and SEM for some thick films before and after friction testing in order to relate the surface morphology to tribological properties. Two types of AFM were used, one was Personal AFM from Burleigh Instruments Inc., and the other was a custom-built instrument with a high stiffness of cantilever beam designed with close control of its metrology for convenience in engineering applications[7]. Most films were measured by the commercial AFM and some also by the large force AFM. At a 'high' contact force around 100 nN, the successive measurements on a poly(pyrrole) film surface show no noticeable distortions, and this indicates that the polymer film is quite tough.

The AFM measurements reveal that poly(pyrrole) films with five counter-ions have a micro-spheroidal morphology. These micro-spheres or 'grains' vary between 0.03 and several micrometres in diameter depending upon the growth conditions. Morphology in general, or specifically the distribution of spheres is more sensitive to the solvent than the counter-ions. For the same counter-ion, the film structure is mainly related to film thickness (below 1 μm). Fig 3 shows AFM images taken from PP/MPA films with a thickness of 0.11, 0.47, 1.4 and 5.2 μm. The scan size is 1.36 $\times$ 1.36 μm^2 for all images but the thickest film, which is 6.8 $\times$ 6.8 μm^2. The thin film tends to have almost spherical features. As the film grows thicker and thicker, more and more spheres tend to agglomerate to form larger, somewhat less regular features, this leads to an average size of features changing from 50 nm in (a) to 100 nm in (b), 250 nm in (c) and 750 nm in (d).

Generally, with the same nominal thickness, the grain size increases with the film type PP/DPA, PP/MPA, PP/TSA, PP/BPA and then PP/DBSA in an order from the smallest to the largest at the level of submicrometres.

The quality of electrode also contributes to film smoothness; wherever a gold substrate was scratched, less uniform films were produced. The scratches seemed to be favourable sites for nucleation leading to isolated mounds of polymer.

In general the AFM measurement alone cannot provide reliable information about the film thickness as it measures the structures at the surface. Average film thickness can be estimated from the nominal area of deposition and the total charge transferred during growth cycling. Films can have the same nominal thickness calculated from the coulometry but possess irregular structures. The combination of these two methods allows a good estimation of the uniformity of a polymer surface.

Results and discussion

Experimental considerations

All specimens were evaluated typically at a loading force of 2 N and a sliding speed of 5 mm s^{-1}, except for the tests on load effect and sliding speed effects. Each data set consists of frictional force, height variation, and sliding speed from the tachometer. A Windows-based data acquisition software was made specially for the tests. All data files contain the same fixed number of data points, with the sample interval preset according to the wearability of a film to give different lengths of test. The frictional force is obtained by measuring the deflection of the spring flexure, and this deflection is relative to its initial position. Ideally this initial position should be at the neutral position of the spring flexure where there is no frictional force acting on the flexure. However, after loading the rotating plate onto the specimen being tested, there is usually an offset due to a residual static friction between the plate and the specimen. This offset can be in any direction and of any value up to the maximum static frictional force, and can cause a significant variation in the measurement. A solution to this is to evaluate the neutral position of the spring flexure by measuring the frictional force in both sliding directions, and then taking the average value. A PTFE bearing pad from Glacier Metal Ltd. was chosen that is in the form of a polymer–metal matrix. The polymer is held in place by a porous sintered bronze layer bonded onto a steel backing plate. The thickness of the complete bearing can be as low as 0.7 mm. The layer thickness of polymer between the bronze and counterface can be reduced to approximately 20 μm by machining the excess layers from the bearing face. The friction coefficient of the PTFE bearing was measured at 0.1 with a standard deviation of 0.005 under a load of 2 N. Using this PTFE bearing, the neutral position of the flexure was measured by rotating the disk in two opposite directions. Due to the low and smooth frictional force of the PTFE bearing, the value thus obtained should be close to the true value. The consequent friction measurements are all based on this value.

For precision slideway applications, both low friction coefficient and small friction variation are of importance, particularly the latter. Therefore three characteristics of a bearing film are monitored. These are the initial running in, steady sliding and stop sliding behaviours. To cover the whole process of the sliding from start to stop, the drive signal from the D/A is designed in a square form which gives 0 V for the first 100 points, then rises to a fixed voltage for mid-range and then drops to 0 V again for the last 100 points. The time interval between two adjacent points can be varied from the data acquisition programme to cope with different sliding distances.

All experiments have been performed in a temperature and humidity controlled metrology laboratory, normally at 20 $\pm$ 1°C and 40 $\pm$ 5% relative humidity.

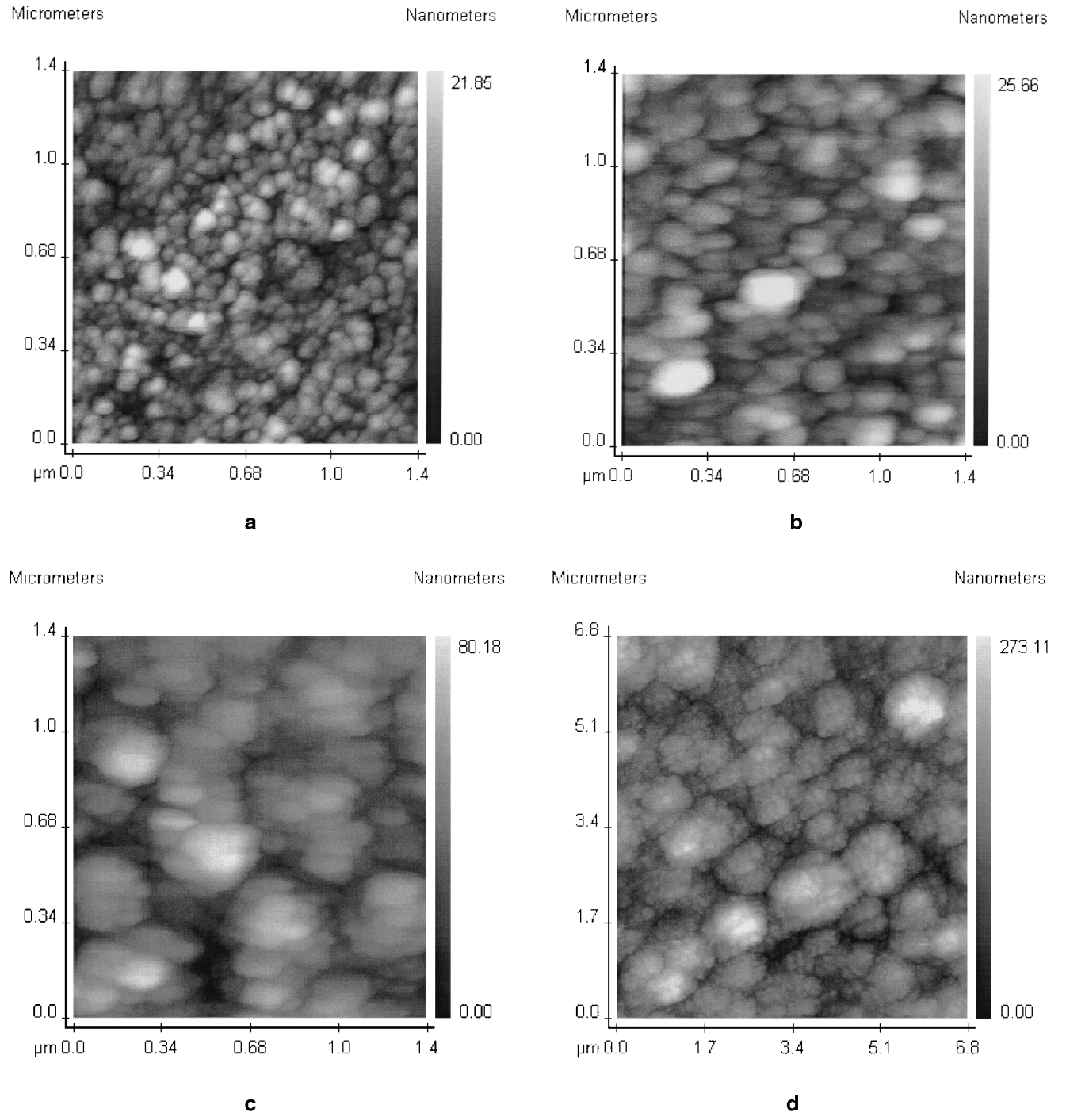

Fig. 3 AFM image of polymer film of PP/MPA with a thickness of (a) 0.11 μm, (b) 0.47 μm, (c) 1.4 μm and (d) 5.2 μm

Measurements of friction and wear

For each test, three signals of frictional force, height variation and sliding speed were simultaneously recorded. The sliding speed is used to evaluate the sliding distance. Fig 4 shows typical plots of the friction coefficient under a normal loading force of 2 N and the height variation of a PP/MPA bearing film. Generally, on the frictional force measurement, there is a high spike at the start point of sliding that is associated with the static friction. After this the friction coefficient rapidly reduces to a fairly steady value, the dynamic friction coefficient. Then the friction drops to a lower value when the sliding stops, sometimes with another spike at the transition. Three parameters are computed from each frictional force measurement, that is the average, the maximum and the standard deviation of friction coefficient. Here the calculation of friction coefficient is based upon the assumption of constant contact force, but in reality this force varies slightly due to the run-out of rotation that also causes stick-slip to take place. Further work is under way to monitor the normal contact force and study the stick-slip behaviour for this particular configuration.

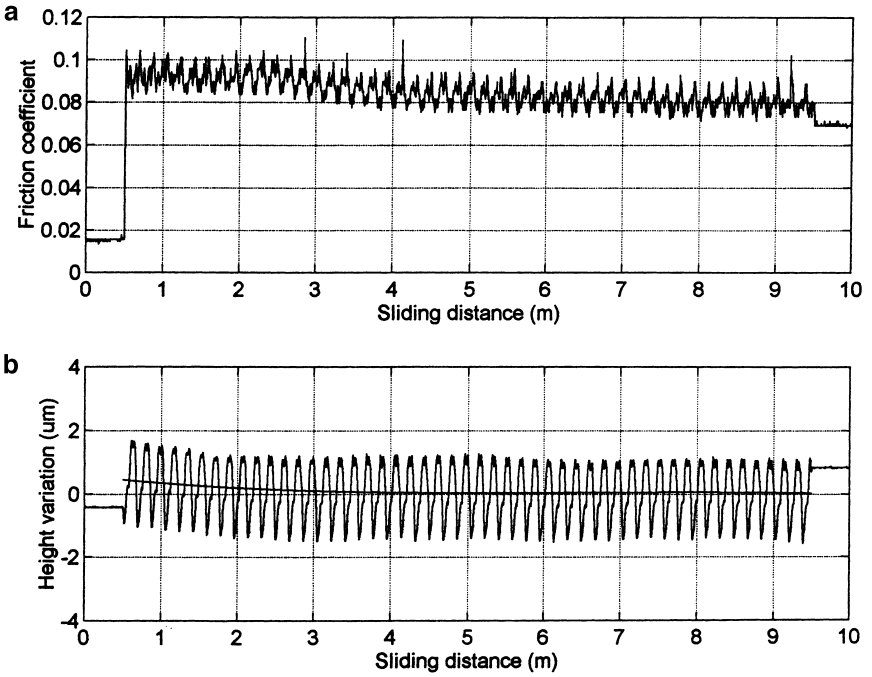

Fig. 4 Measurements of (a) friction coefficient and (b) wear rate of a PP/TSA film under a load of 2 N and a sliding speed of 5 mm s^{-1}

The height variation has two distinguished patterns: one is modulated by the surface roughness and run-out of the rotating disk, and the other is caused by the wear of the film being tested. The former is a systematic error signal with a frequency corresponding to the rotation speed of the motor, and the latter is an almost DC signal that corresponds to the wear of the film. The wear rate is obtained via data regression to find the latter signal, in our case using 'Matlab'. Due to the large data sets used, normally 7200 that cover many cycles, the oscillating signal has little effect on the regressed result. Here we take 'wear' as the functional property determining bearing life, whether the actual cause is material removal or, for example, redistribution out of the contact region. Generally, the poly(pyrrole) films have a wear rate of a few nanometres per millimetre sliding. Some, particularly PP/TSA and PP/DPA, offer a rate close to or slightly better than that of PTFE, which is claimed to be about 0.1 nm/mm[8] but was measured at 0.2 nm/mm with the PTFE bearing used here.

The main sequence of the systematic tests has confirmed and added confidence to the preliminary results reported earlier[5]. Fig 5 shows the range of friction coefficient values observed from poly(pyrrole) (PP) with five counter-ions: MPA, DPA, BPA, DBSA and TSA. Friction coefficients in the range 0.05 to 0.1 (similar to PTFE) are observed with some pyrrole-based films, particularly PP/MPA and PP/TSA. In general, friction coefficients vary widely with PP/DBSA, PP/BPA and PP/TSA groups but only modestly with PP/DPA and PP/MPA, so this property of the latter films can be more easily controlled.

The measured wear rates for different bearing specimens are shown in Fig 6(a). The most interesting region on this graph is the lower corner on the left

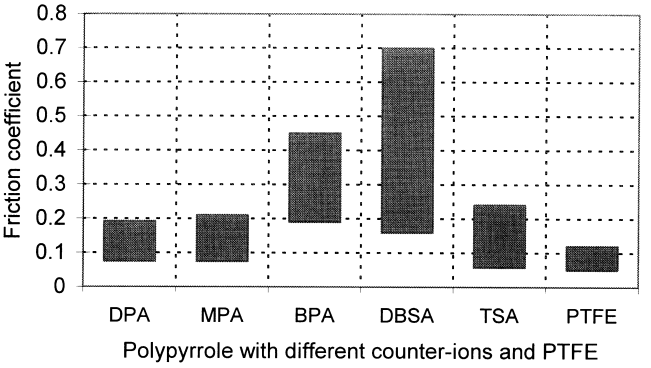

Fig. 5 Range of achievable dynamic friction coefficient for poly(pyrrole) specimens and PTFE

because it represents low friction and low wear-rate. Most poly(pyrrole) films are in a region between 0.1 and 0.2 for friction coefficient and 0.1 and 1 nm/mm for wear-rate, except for PP/DBSA films, which have higher friction coefficients but relatively lower wear rates. With sub-micrometer films on smooth substrates even these low rates mean that bearings wear out over quite small total distances. It is known that baking the films at a moderately high temperature both drives off residual solvent and increases the thermodynamic stability of the polymer. It is plausible that the effect on mechanical behaviour is also significant and so some specimens were baked in an oven for about 12 h in the hope of improving film durability. The study shows that, statistically, there is an improvement in the wear resistance but also an increase in friction, as shown in Fig 6(b) where all specimens were grown under nominally the same conditions with a film thickness 0.5 μm but half of them were baked at 200°C. The effect of the high temperature treatment could be

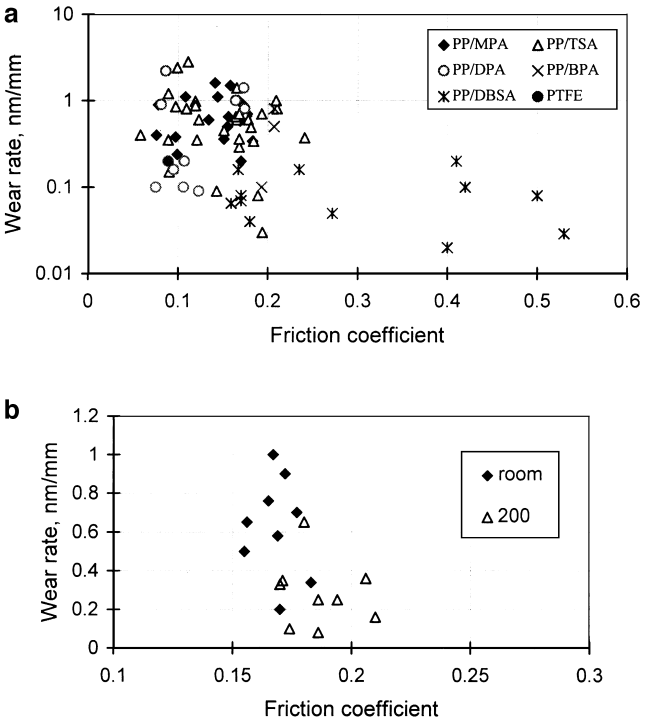

Fig. 6 (a) Wear rate against dynamic friction coefficient for different bearing specimens. (b) Effect of heat treatment on tribological properties for PP/MPA films

the result of the rearrangement of surface topography, leading to a smoother surface with stronger bonding force between polymer spheres. Some specimens of PP/MPA with a thickness of less than 0.2 μm changed colour from a dark blue to yellow/gold on baking. Since the thickness is of the order of the wavelength of light this is probably caused by a complex interaction of changes in oxidation (affecting optical properties) and some changes in film density and thickness due to the curved surface shape.

Effects of growth conditions

In addition to the counter-ion, the friction coefficient of a polymer film is also affected by a number of other factors such as growth potential, film thickness and surface topographies of both the film and the substrate. The influence of growth potential has been tested by applying different combinations of initial step potential and final potential to the polymerisation process. Generally, there is a reduction in friction with the double step growth potential. The AFM measurements show that such a specimen normally has a more uniformly distributed surface. Our measurements indicate that the friction coefficient reaches a minimum value at a specific film thickness. In the thin film limit, asperities of the substrate break through the film and the shear stress of the substrate increases the friction coefficient. In the thick film limit, the friction coefficient may be increased by large contact area and ploughing of the film. Fig 7 shows the dependence of friction coefficient on film thickness with three types of polymers, PP/TSA, PP/MPA and PP/DPA. There exists a general trend that friction coefficient is high

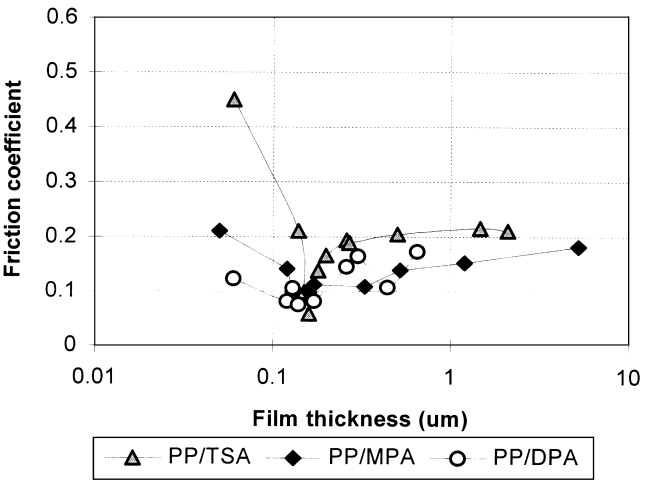

Fig. 7 The effect of film thickness on friction coefficient

for very thin films < 0.1 μm, decreases sharply to a minimum at a thickness around $0.14 \sim 0.16$ μm, then increases steadily and finally stabilises at thicker films. The fluctuation in friction coefficient within specimens is higher for thin films than thick films, and higher for PP/TSA than PP/DPA and PP/MPA. Here the film thickness is estimated from the nominal area of deposition and the total charge transferred during the growth or background cycling. However, in practice there are a number of factors influencing film thickness such as potential distribution, contaminants on the electrode and the topography of substrate, which makes the growth process less predictable and leads to variation in friction coefficient. Thus it is necessary to combine film topography with the average film thickness to give a good estimation of the uniformity of a polymer surface. Attempts have been made to correlate the film topography with its frictional behaviour and results are reported elsewhere[9]. For a given nominal film thickness, 0.5 μm in this case, the friction coefficient of the bearing specimens produced from batch to batch is 0.17 ± 0.01 for PP/TSA and 0.18 ± 0.02 for PP/MPA.

The lifetime variation of the friction coefficient for a polymer film was tested and a typical result is plotted in Fig 8, which shows the variation of friction coefficient against the sliding distance for the specimen of

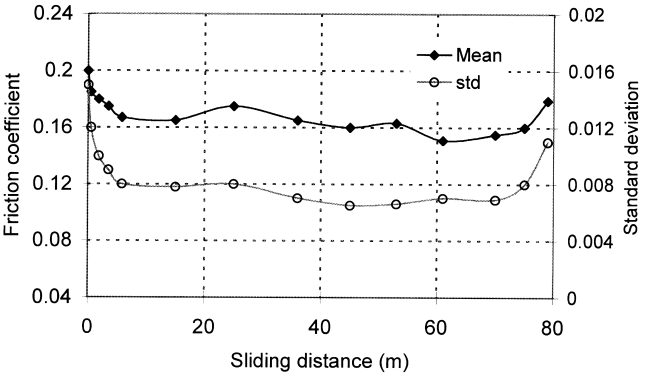

Fig. 8 Variation of dynamic friction coefficient against sliding distance for PP/TSA with a nominal thickness of 1.4 μm

PP/TSA with a nominal thickness of 5.2 μm. The lifetime variation of friction coefficient of this particular type of bearing specimens is less than 30%.

Effect of loading force

The frictional force between two sliding surfaces can be expressed by the simple model

$$F = AS + F_p \tag{1}$$

where A is the area of contact, S is the shear strength of the interface, and F_p is the ploughing term. To reduce friction, the shear strength, the contact area and the ploughing contribution have to be minimised. The reason that film lubrication reduces friction is that a hard substrate reduces both the area of contact and the penetration (the ploughing) while a soft film reduces the shear strength. The friction coefficient, μ, is obtained by dividing the frictional force by the normal load, L. For thin films the ploughing term can be ignored, and then the friction coefficient is given by

$$\mu = F/L = AS/L = S/P \tag{2}$$

The shear strength of solids at high pressure has been observed[10] to have a pressure dependence, approximately

$$S = S_0 + \alpha P \tag{3}$$

where α represents the pressure dependence of the shear strength. S_0 is the intrinsic shear strength of the solid. Substituting Equation (3) into Equation (2) gives the friction coefficient as:

$$\mu = S_0/P + \alpha \tag{4}$$
$$= S_0 A L^{-1} + \alpha$$

Using Hertzian theory to estimate A, the friction coefficient, for smooth balls and flat substrates loaded below the elastic limit (typical of bearing design), is then

$$\mu = \pi S_0 \left(\frac{3R}{4E}\right)^{2/3} L^{-1/3} + \alpha \tag{5}$$

where E is the composite elastic modulus of the sliding pair, R is the radius of the ball, and L is the normal load. The friction coefficient is proportional to $L^{-1/3}$ for ball-on-flat contact and tends asymptotically towards α as the load increases.

Three different bearing materials were tested under a loading force varying from 0.1 to 5 N. They are PTFE, PP/MPA and PP/TSA. The results are plotted in Fig 9(a–c). Here 'data' indicates the measured mean dynamic friction coefficient at each load, 'theoretical' shows the result when the data points are regressed to $L^{-1/3}$, that is $\mu = cL^{-1/3} + \alpha$, and 'best fit' shows the best fitting curve. The latter uses a non-linear fitting algorithm to search for an optimal value b to get the minimum fitting error (assessed as sum of squares of residuals) in the formula $\mu = c_1 L^b + \alpha$. The friction coefficient vs. load for PTFE exhibited roughly the $L^{-1/3}$ behaviour expected for ball-on-flat geometry in general, although the best fit curves show a dependence close to L^{-1} for other materials ($b = -0.99$ for PP/MPA and $b = -0.83$ for PP/TSA compared with -0.45 for PTFE). The reason of this near inverse proportionality is not yet clear. It is unlikely to be an artifact due to the limited number of data points and/or measurement error. The error in the measurement of frictional force can be estimated from the first 100 points in each data (see Fig 4), which represents the pre-sliding status and the standard deviation of the non-sliding signal is about 0.0004. It is about 10 times better than the smoothest bearing with PTFE (0.005). Although the accuracy of any individual data point, determined principally by the setting of load and load-cell calibration, may vary by 5% it will do so randomly. The systematic variation between materials is a genuine effect. The higher values of the coefficient b for PP/MPA and PP/TSA are probably due to the fact that the conductive films studied here are much thinner than PTFE films, in both cases the film thickness was 0.5 μm. Under these conditions, thermal effects or flow due to the high local stress may behave differently. Tests were also carried out on films with different thickness and the results show a

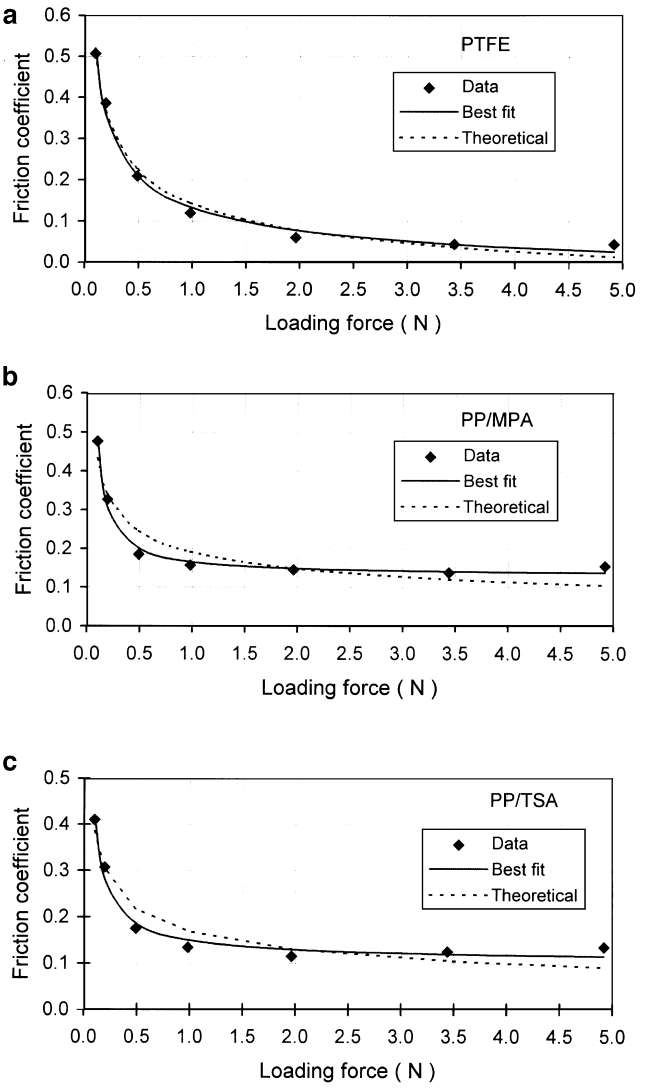

Fig. 9 (a) Effect of load on dynamic friction coefficient for PTFE bearing. (b) Effect of load on dynamic friction coefficient for PP/MPA bearing. (c) Effect of load on dynamic friction coefficient for PP/TSA bearing

similar trend. The poly(pyrrole) films of both PP/MPA and PP/TSA show a rapid reduction on the friction coefficient at low loads but give a near constant friction coefficient for loads higher than 1 N. This is in contrast with PTFE which shows a steady decrease on friction coefficient at higher loads. The fairly consistent friction coefficient under a range of loading forces from 1 to 5 N shown by poly(pyrrole) films is useful for applications in precision slideways.

Effect of sliding speed

For precision slideway applications the bearing should have consistent behaviour at sliding speeds up to a few tens of mm s^{-1}. To test the effect of sliding speed on friction, two ramp voltage signals were used, one continuously increased the motor speed from zero to 28 mm s^{-1} then reduced steadily back to zero, the other was a step increased ramp. Tests were carried out on the PTFE and PP/MPA bearings, and two typical results are plotted in Fig 10(a,b). In general, the friction coefficient is high at very low speeds, decreases rapidly as the speed increases, reaches a minimum at around 10 mm s^{-1} for PTFE and 2 mm s^{-2} for PP/MPA, then slowly increases to a steady value of 0.07 for PTFE, and 0.17 for PP/MPA. When the speed decreases during the reverse ramp, the friction coefficient for both bearing materials shows a slow and steady decrease throughout the speed range. The reasons for this speed effect on the frictional characteristics are unclear, but may be related to strain-rate sensitivity or a temperature effect at the contact spot[11]. It may be more appropriate to assume that the adhesion junction formed at the contact is time-dependent as originally proposed by Sampson *et al.*[12], strengthening with increased contact time, as this could correlate with higher energy loss in low-speed sliding. Recently Thompson and Robbins[13] proposed that at any instant during sliding the friction at any local region is always a combination of static (sticking) and kinetic (sliding) friction components. More time will be spent in sliding than sticking as the speed increases, thus the overall friction coefficient falls. However, this cannot explain, particularly for PP/MPA films, why the friction coefficient rises again at a higher sliding speed and stabilises after 10 mm s^{-1} while the PTFE bearing shows no significant increase. This could be caused by temperature increase at the contact due to different thermal capacity for these two type of specimen configurations. The PP/MPA film (~12 $mm^2 \times 1$ μm) is on a glass substrate while the PTFE composite film is on a steel backing plate with a volume about 60 $mm^2 \times 1$ mm. Therefore, a much higher temperature rise would be expected for the PP/MPA film than the PTFE. Further work is needed to investigate the temperature effect in conjunction with the sliding speed effect by monitoring the temperature change at the contact spot.

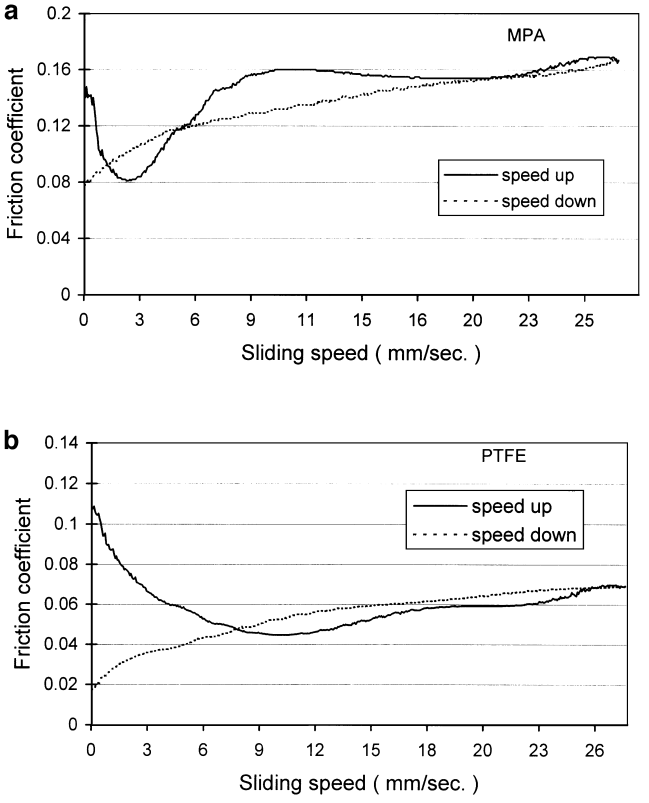

Fig. 10 (a) Effect of sliding speed on dynamic friction coefficient for PP/MPA in a speed range up to 28 mm s^{-1}. (b) Effect of sliding speed on dynamic friction coefficient for PTFE

Conclusions

Over 200 specimens of poly(pyrrole) films grown under different conditions have been tested usnig special instrumentation that provides simultaneous measurements of friction and wear rate with resolutions of 100 μN for frictional force and 2 nm for height variation. This has shown that a wide range of tribological properties can be selected for different applications. Characterisation of the structure of these polymer films has been carried out by AFM which helps to evaluate the effect of the polymerisation process. The tribological properties of these polymer bearings vary under the influence of a variable contact force and sliding speed as broadly expected but differ in exact form from existing models of behaviour. Further work is being carried out to examine this anomaly and to study the effects of humidity, temperature, higher speeds and higher loads on friction and wear. The testing to date indicates that poly(pyrrole) dry bearings have potential applications in instrument systems where loads and duty cycles tend to be low and where PTFE is difficult to apply. The continuing programme will reveal whether they are also effective for a wide range of precision machine or micro-mechanical applications.

Acknowledgements

The authors would like to thank Dr S. Spraggette of the School of Engineering, Coventry University, for his support and technicians at the Center for Nanotechnology and Microengineering at the University of Warwick and the AFM/SEM laboratory at Coventry University. Some of this work was generously supported by the UK Engineering and Physical Science Research Council under grant GR/H36382. Support from Coventry University Research Fund is greatly appreciated.

References

1. Clechet, P., Martelet, C., Belin, M., Zarrad, H., Jaffrezic-Renault, N. and Fayeulle, S., *Sensors and Actuators A*, 1994, **44**, 77–81.
2. Bhushan, B., *Tribology and Mechanics of Magnetic Storage Devices*. Springer, New York, 1990.
3. Lindsey, K., Smith, S. T. and Robbie, C. J., Sub-nanometre surface texture and profile measurement with Nanosurf 2. *Ann. CIRP*, 1988, **37**, 519–522.
4. Smith, S. T., Harb, S. and Chetwynd, D. G., Tribological properties of polymeric bearings at the nanometre level. *J. Phys. D.*, 1992, **25**(1A), 240–248.
5. Smith, S. T., Harb, S., Eastwick-Field, V., Yao, Z. Q., Bartlett, P. N., Chetwynd, D. G. and Gardner, J. W., Tribological properties of electroactive polymeric thin film bearings. *Wear*, 1993, **169**, 43–57.
6. Gardner, J. W., Chetwynd, D. G., Smith, S. T., Harb, S., Yao, Z. Q., Bartlett, P. N. and Eastwick-Field, V., Electropolymerized films for low friction microactuator bearings. *Sensors and Actuators A*, 1994, **41/42**, 300–303.
7. Xu, Y., Smith, S. T., Atherton, P. D., Judge, T. and Jones, R., A. metrological scanning force microscope. In *Proceedings of ASPE 9th Annual Meeting*. Cincinnati, USA, 1994, pp. 23–28.
8. Tanaka, K., Uchiyama, Y. and Toyooka, S., The mechanism of wear of the polytetrafluoroethylene. *Wear*, 1973, **23**, 153–172.
9. Liu, X., Chetwynd, D. G. and Gardner, J. W., Surface characterisation of electroactive thin polymer film bearings. *Int. J. Mach. Tools and Manuf.*, 1998, **38**(5/6), 669–675.
10. Singer, I. L., Solid lubrication processes. In *Fundamentals of Friction: Macroscopic and Microscopic Processes*, ed. I. L. Singer and H. M. Pollock. NATO ASI series, Kluwer Academic Publisher, London, 1990, pp. 237–261.
11. Briscoe, B. J., Friction of organic polymers. In *Fundamentals of Friction: Macroscopic and Microscopic Processes*, ed. I. L. Singer and H. M. Pollock. NATO ASI series, Kluwer Academic Publisher, London, 1990, pp. 167–181.
12. Sampson, J. B., Morgan, F., Reed, D. W. and Muskat, M., Studies in lubrication XII. Friction behaviour during the slip portion of the stick–slip process. *J. Appl. Phys.*, 1943, **14**, 689–799.
13. Thompson, P. A. and Robbins, M. O., Origin of stick–slip motion in boundary lubrication. *Science*, 1990, **250**, 792–794.